# Chapter 14
# Using Minimum Entropy Decomposition for Rolling Element Bearing Fault Diagnosis in a Permanent Magnet Motor

**Surendra (Suri) Ganeriwala**

**Abstract** The rolling element bearing is one of the most vulnerable components in a permanent magnet motor because it is most often under high load and high-speed running conditions. Prompt diagnostics of rolling element bearing faults is critical not only for the safe operation of machines, but also for the reduction of maintenance cost. This work studies the diagnostics of bearing inner race and outer race faults. Rolling element bearing fault diagnosis using vibration signals relies profoundly on using the well-developed methodology of envelope analysis. Envelope analysis is traditionally performed by amplitude demodulating an excited frequency band using Hilbert transformation to determine the fault frequencies. The enveloping technique suffers due to a low signal-to-noise ratio and not knowing the frequency band where to apply it. In this paper we present the fault analysis results of bearing with inner race and outer race defects in a permanent magnet motor using traditional enveloping combined with advanced signal processing techniques. Minimum Entropy Decomposition (MED) is used to enhance bearing signal in cases with a low signal-to-noise ratio. Spectral Kurtosis (SK) is used to identify the demodulation band. Results show that the efficiency of the envelope analysis in providing a correct diagnosis is increased when it is augmented with bearing signal enhancing and frequency band determination techniques.

**Keywords** Outer race bearing fault · Inner race bearing fault · Minimum entropy deconvolution · Spectral kurtosis · Envelop analysis

## Introduction

The rolling element bearing is widely used in today's rotating machinery. Unlike the long-life fluid bearing, the rolling element bearing often encounters metal-to-metal contacts under high load and high-speed running conditions, which makes it one of the most vulnerable components in a machine. Diagnostics of rolling element bearing faults can guarantee safe operation of the machine and reduce the maintenance cost. Faults usually occur on the four main components of a rolling element bearing, i.e., the outer race, the inner race, the ball, and the cage. Hence, it is crucial to detect the corresponding fault frequencies, i.e., ball pass frequency outer race (BPFO), ball pass frequency inner race (BPFI), ball spin frequency (BSF), and fundamental train frequency (FTF) [1, 2]. The values of them are determined by the geometry of the bearing and the rotating speed of the shaft.

When a local fault occurs in a bearing, a series of impacts are generated when the rollers or balls rolling over the fault. Like a hammer test in modal analysis, these impacts will excite the high frequency resonances of the machine. Depending on the location of the fault, different features of the vibration signal are generated by the fault, as shown in Figure 1. The outer race fault usually occurs in the load zone and are not modulated by any rotating speed. In contrast, the inner race fault is typically modulated by the shaft speed and the impact has the largest amplitude when the fault passes the load zone. Like the inner race fault, the rolling element ball fault is modulated by the FTF.

Surendra (Suri) Ganeriwala
Spectra Quest, Inc., Richmond, VA 23228
e-mail: suri@spectraquest.com

© The Author(s), under exclusive license to River Publishers 2026
Kristin B. Zimmerman, PhD (eds.), *Special Topics & Experimental Techniques in Structural Dynamics, 2026, Vol. 5*, Conference Proceedings of the Society for Experimental Mechanics Series, https://doi.org/10.13052/rp-9788743814160

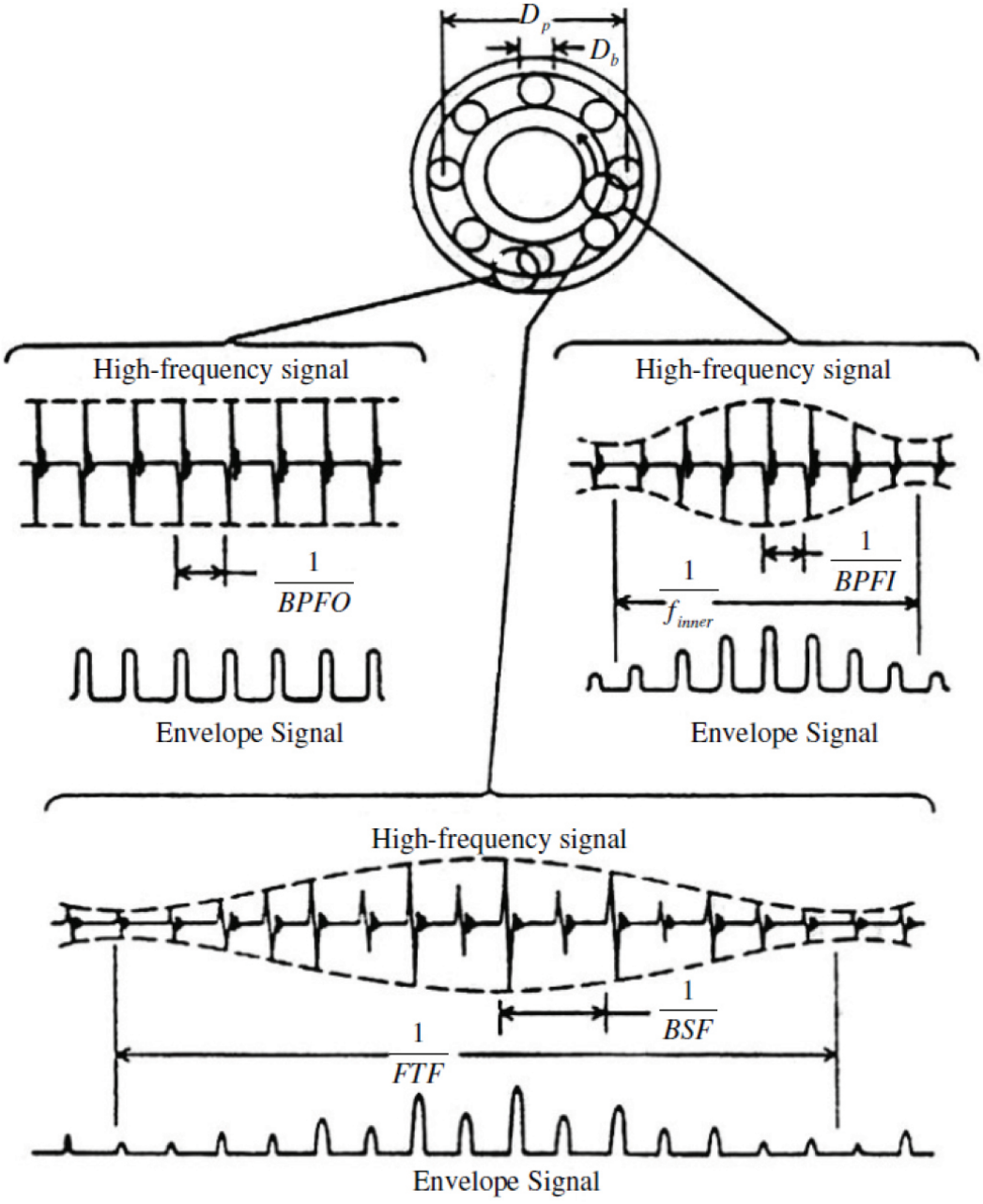



**Fig. 1** Features of vibration signals generated by different locations of a fault in a rolling element bearing (stationary outer race) [3]

## *Envelope Analysis*

In order to detect the bearing fault frequencies from a vibration signal measured by an accelerometer, envelope analysis is the main method to be applied. For a measured vibration signal $y(t)$, the first step of envelope analysis is to perform complex demodulation of the signal, which can be obtained by

$$Y(t) = y(t)exp(\ -jp(f_l + f_u)t) \tag{1}$$

where $f_l$ and $f_u$ are the lower and upper limits of a selected frequency band. The second step is to lowpass filter the demodulated signal $Y(t)$ to compute the analytic signal $z(t)$. The cutoff frequency of the lowpass filter is $(f_u - f_l)/2$.

### *Minimum Entropy Deconvolution (MED)*

One can see that the selection of a proper frequency band is the key of envelope analysis. For a rotating machinery, besides the bearing fault frequencies, there are other frequency components in the vibration signal, especially the rotating frequency and its harmonics. Those discrete frequency components contain the major energy in the signal and could mask the bearing fault frequencies, especially in the early stage of the bearing fault, which causes some difficulty to choose the proper frequency band. Hence, it is important to separate those discrete frequency components first. A lot of signal processing methods have been investigated for this purpose, such as time synchronization averaging, cepstrum, and adaptive filtering [4]. They require extra efforts to process the signal and are not in the scope of this paper. Since the vibration signal is measured by an accelerometer on the housing of a bearing instead of directly from the bearing, the transfer path from bearing to the accelerometer also has an effect on the acquired signal, such as reducing the amplitude of the impact generated by the bearing fault. In order to minimize the effect from the transfer path, the MED technique is used here [5, 6]. The output of a linear time-invariant system can be expressed as the convolution integral of the system input and system's impulse response

$$y(t) = x(t) * h(t) = \int_{-8}^{8} h(t-t)x(t)dt \tag{2}$$

where $y(t)$ is the measured output signal, $x(t)$ is the original signal from the bearing, and $h(t)$ is the impulse response of the system. The deconvolution is to find an inverse filter to remove the effect of $h(t)$ and recover the original signal $x(t)$. In order to obtain the coefficients of the optimal filter, an optimization problem based on kurtosis is formulated. Kurtosis is a measure of "peakedness" of a signal. Since a series of impacts are generated by the local fault of the bearing, the optimization problem is to maximize the kurtosis of the output signal $y(t)$. More details on the MED technique can be found in Ref. [5].

### *Spectral Kurtosis (SK)*

After the kurtosis of the vibration signal is maximized by the MED technique, a proper frequency band can be selected through the SK using a kurtogram [7, 8]. The SK can indicate the nonstationary or non-Gaussian frequency components of the signal in the frequency domain. In the kurtogram, small values of SK can be seen at frequencies where only stationary Gaussian noise exists, while large values of SK can be seen at frequencies where transient occurs. The SK of a signal $y(t)$ can be computed based on the short-time Fourier transform (STFT) of the signal

$$S(t,f) = \int_{-8}^{8} y(t)w(t-t)e^{-2pft}dt \tag{3}$$

where $w(t)$ is the window function used in STFT. The SK is calculated by

$$SK(f) = \frac{\left(\sum_{i=1}^{n} |S(t_i,f)|^4\right)/n}{\left(\left(\sum_{i=1}^{n} |S(t_i,f)|^2\right)/n\right)^2} - 2, f?0 \tag{4}$$

STFT-based kurtogram is associated with constant time and frequency resolution. Sawalhi [3] used complex Morlet wavelets to construct different filter banks to calculate kurtogram. The wavelets have the property of uniform resolution on a logarithmic frequency scale. Antoni [9] proposed a fast kurtogram algorithm using bandpass filtering along with a simplified computation to approximate the SK for each window size and frequency rather than compute the STFT, which makes it more suitable for on-line industrial applications. This paper will use the fast algorithm to calculate kurtogram.

## Experimental Investigation

Experiments were conducted on a drive-train diagnostics/prognostics test rig, as shown in Figure 2. This test rig can be used to study the transmission diagnostics/prognostics and gear dynamics. One bearing on the drive motor was seeded with outer race fault and inner race fault separately. The bearing information is shown in Table 1. Two single-axis accelerometers that were used to measure horizontal and vertical vibration were mounted on the housing of the motor, as shown in Figure 3. One can see that there is a transfer path between the bearing and actual measurement location. The bearing fault analysis were investigated at three rotating speeds, including 1800 RPM, 3600 RPM and 5000 RPM. Corresponding bearing fault frequencies are shown in Table 2. The data was acquired by SpectraQuest DAQ and in-house software VibraQuest. The sampling frequency was 102.4 kHz and the acquisition time was 12.8 s. Vibration data in the vertical direction is used for analysis in the following sections.

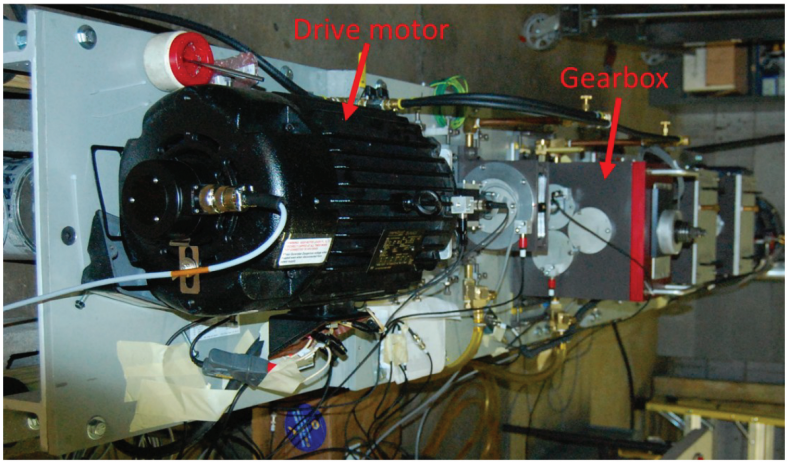



**Fig. 2** Drive-train diagnostics/prognostics test rig

**Table 1** Bearing information

| Bearing | # of rolling elements | Pitch diameter | Rolling element diameter | Contact angle |
|---|---|---|---|---|
| 6307 | 8 | 2.264 in | 0.531 in | 0 degree |

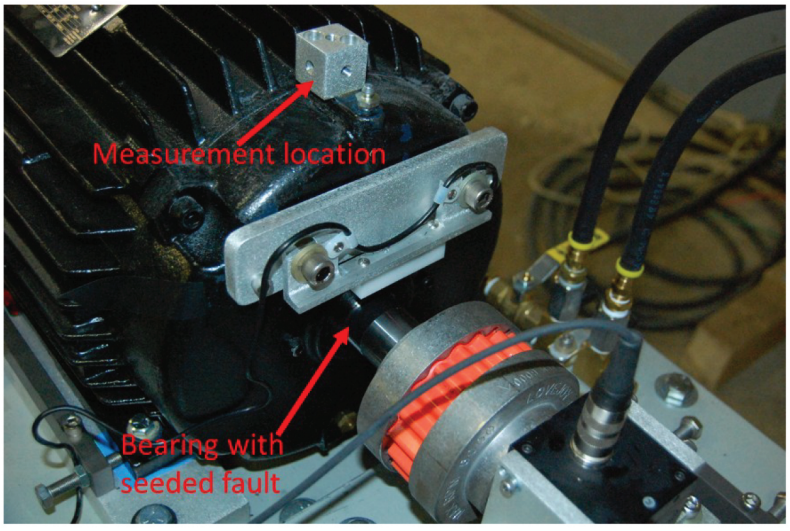



**Fig. 3** Faulted rolling element bearing and measurement location

**Table 2** Bearing fault frequencies at different rotating speeds

| Rotating Speed | BPFO | BPFI | BSF | FTF |
|---|---|---|---|---|
| 1800 RPM | 91.855 Hz | 148.145 Hz | 60.437 Hz | 11.482 Hz |
| 3600 RPM | 183.710 Hz | 296.290 Hz | 120.873 Hz | 22.964 Hz |
| 5000 RPM | 255.153 Hz | 411.514 Hz | 167.880 Hz | 31.894 Hz |

### *Outer Race Fault*

The raw vertical vibration data between 0 s and 0.1 s at the three rotating speeds are shown in Figure 4. A series of impacts corresponding to the BPFO can be seen in Figure 4(a) at the rotating speed of 1800 RPM, though not very prominent. As the rotating speed increases, the impacts are less prominent and are mixed with general vibration. The raw data was then processed by the MED technique, and the results are shown in Figure 4. Compared to Figure 4(a), the impacts in Figure 4(a) are more prominent, which makes it easier to identify the corresponding BPFO. Appearance of the impacts in Figure 4(b) and (c) is also improved. From Figures 4 and 5, one can see that the transfer path from the bearing to the measurement

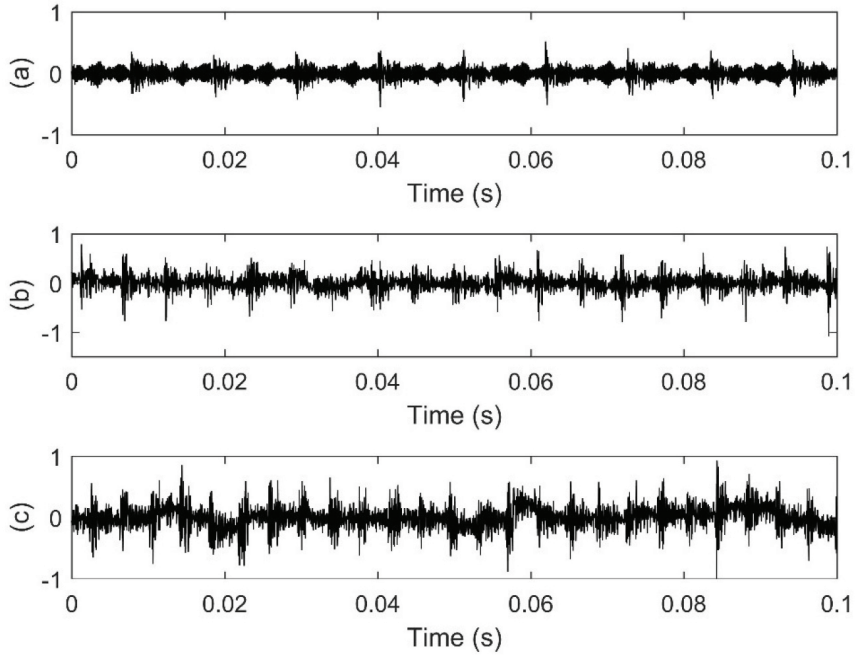



**Fig. 4** Raw vertical vibration data corresponding to the outer race fault at (a) 1800 RPM, (b) 3600 RPM and (c) 5000 RPM

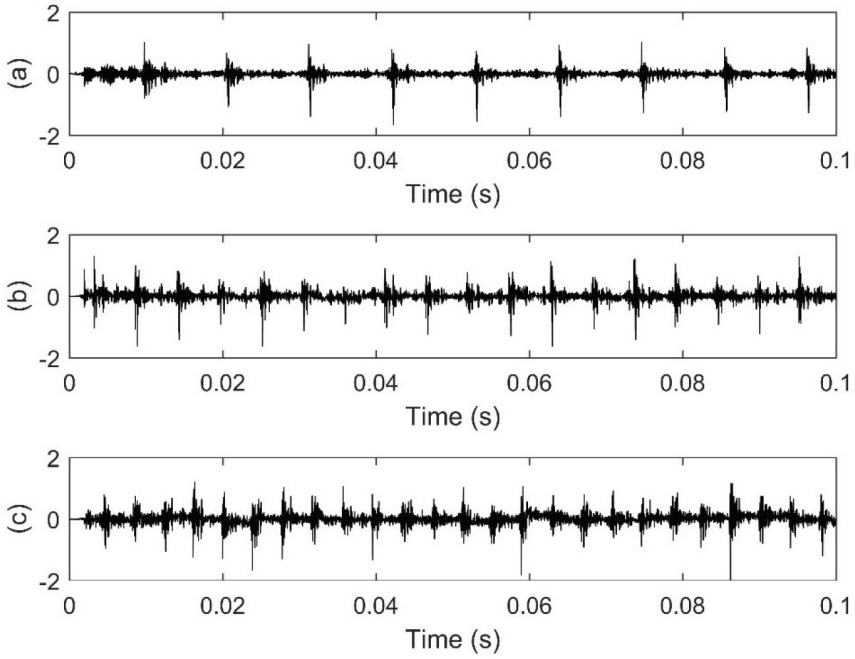



**Fig. 5** Data processed by the MED technique at (a) 1800 RPM, (b) 3600 RPM and (c) 5000 RPM

location has a negative effect on the impacts generated by the bearing fault and the MED technique can reduce this negative effect. The kurtosis was calculated before and after applying the MED technique and is shown in Table 3. One can see that the kurtosis is greatly increased after applying the MED technique at all the three rotating speeds. Since the kurtosis is a measure of "peakedness", larger kurtosis indicates more obvious "peakedness" in the data, which agrees well with the results in Figure 5.

Kurtogram of the processed data is shown in Figure 6 and Figure 7, respectively. The proper frequency band for envelope analysis can be obtained from the kurtogram. The amplitude spectrum of the envelop signal was calculated using the frequency band obtained from the kurtogram by each method, as shown in Figures 6 and 7. Though the proper frequency bands obtained by the two methods are different, the BPFO and its harmonics can be clearly identified at each rotating speed in Figures 6 and 7. Since this is an outer race fault, there is no sideband around the BPFO.

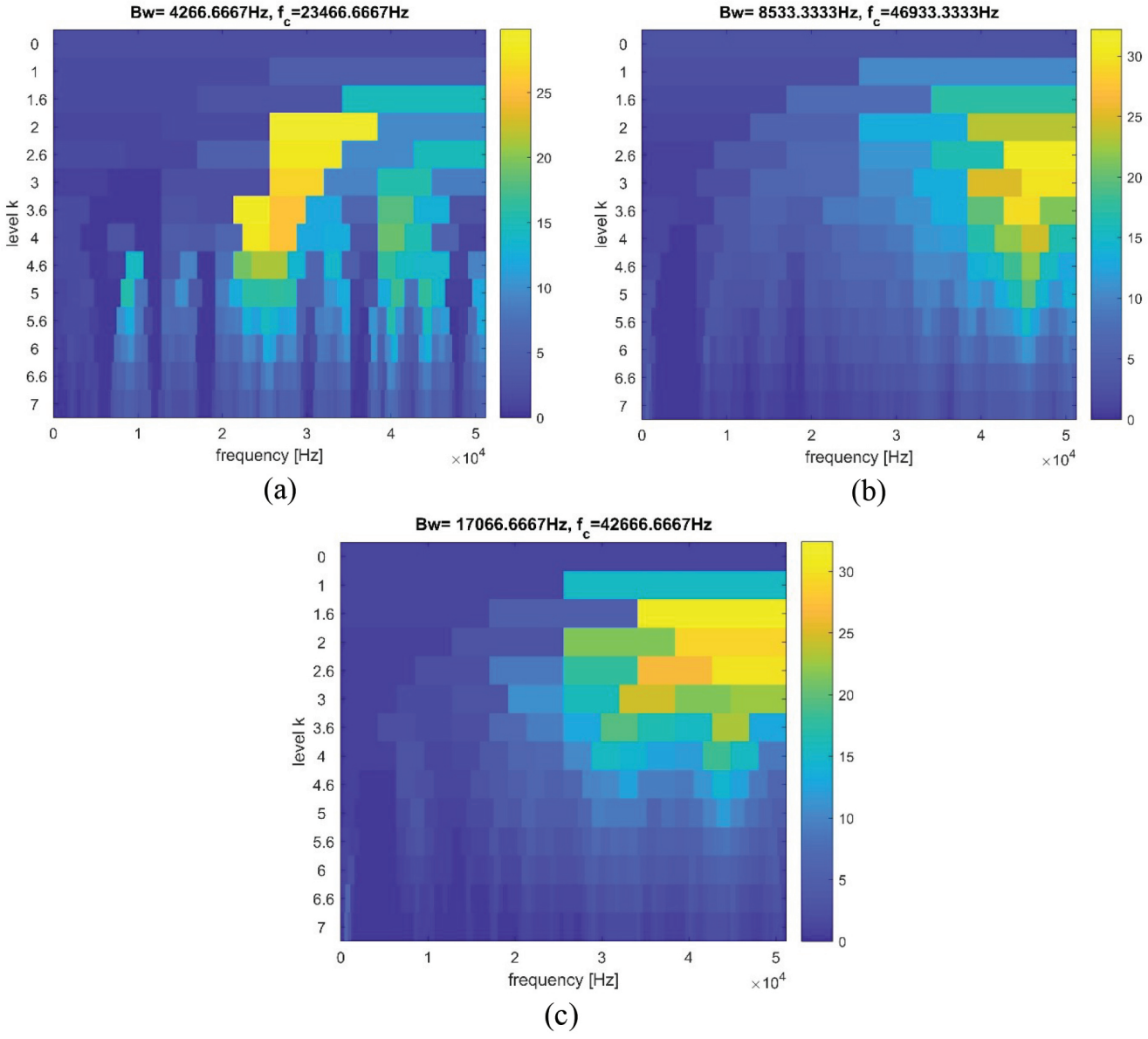



**Fig. 6** Kurtogram corresponding to the outer race fault at (a) 1800 RPM, (b) 3600 RPM and (c) 5000 RPM calculated by the fast algorithm

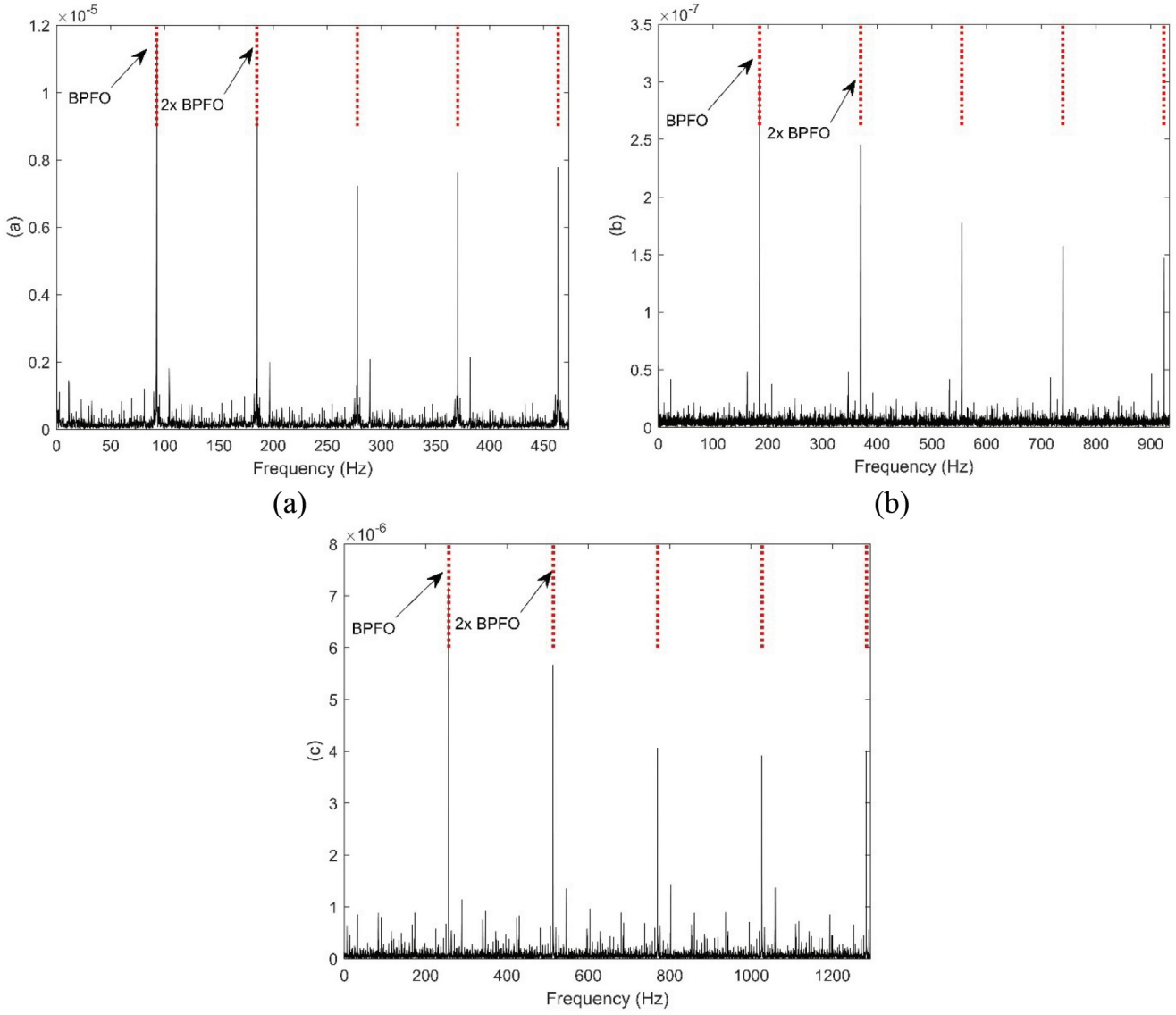



**Fig. 7** Amplitude spectrum of the square envelope signal from the fast algorithm corresponding to the outer race fault at (a) 1800 RPM, (b) 3600 RPM and (c) 5000 RPM

**Table 3** Kurtosis before and after applying the MED technique

| Rotating Speed | Before | After |
|---|---|---|
| 1800 RPM | 3.0254 | 42.5602 |
| 3600 RPM | 3.8301 | 16.5063 |
| 5000 RPM | 2.3856 | 8.7642 |

## *Inner Race Fault*

The raw vertical vibration data corresponding to the inner race fault is shown in Figure 8. It is difficult to tell the location of an impact in Figure 8(a). Some impacts can be seen in Figure 8(b) and (c). The effect of amplitude modulation by the rotating shaft is not obvious. The raw data was then processed by the MED technique and is shown in Figure 9. One can see that the impacts are more obvious in the processed data compared to those in the raw data. The kurtosis was calculated before and after applying the MED technique and is shown in Table 4. One can see that the kurtosis is slightly increased, but

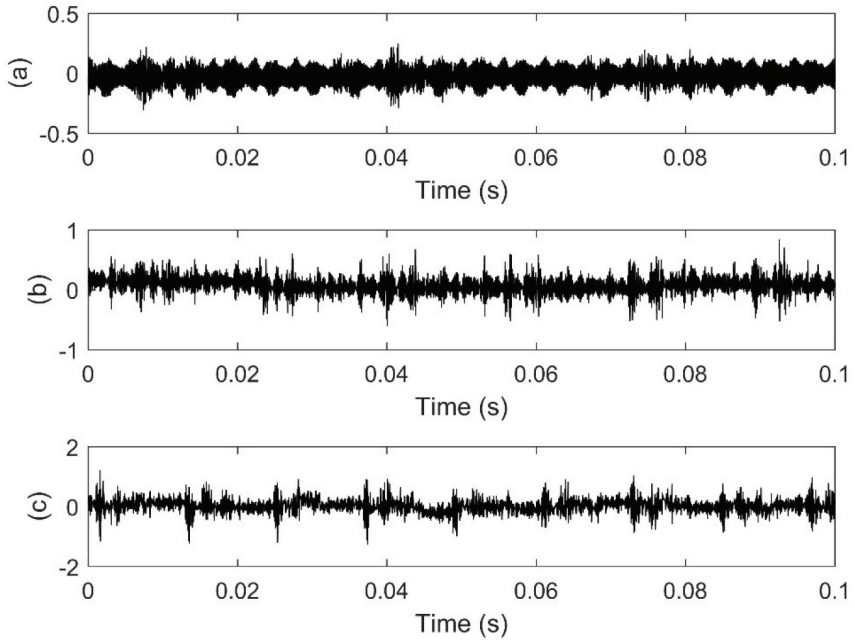



**Fig. 8** Raw vertical vibration data corresponding to the inner race fault at (a) 1800 RPM, (b) 3600 RPM and (c) 5000 RPM

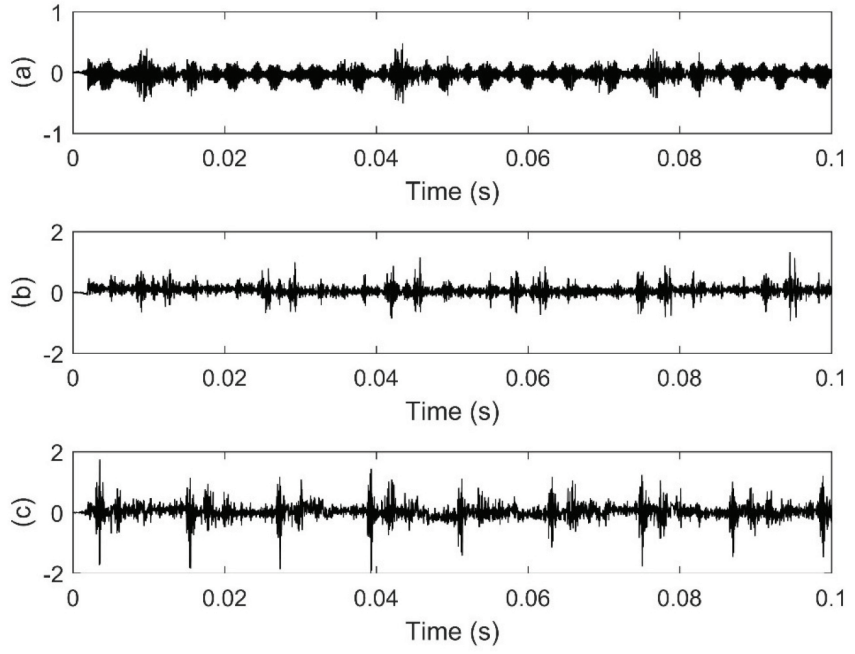



**Fig. 9** Data processed by the MED technique at (a) 1800 RPM, (b) 3600 RPM and (c) 5000 RPM

**Table 4** Kurtosis before and after applying the MED technique

| Rotating Speed | Before | After |
|---|---|---|
| 1800 RPM | 0.5715 | 4.1604 |
| 3600 RPM | 1.6744 | 4.5812 |
| 5000 RPM | 3.2212 | 6.8436 |

not as much as the case in Sec. 2.1. One possible reason is that the transfer path in this case has more components involved since the fault is from inner race. Impacts generated by the inner race fault is weaker at the measurement location.

Kurtogram of the processed data is shown in Figures 8 and 9. One can see that the bandwidths are narrower than those in Sec. 2.1, which indicates that the energy of the impacts generated by the inner race fault is smaller. The frequency bands obtained from the two methods are similar at 3600 RPM and 5000 RPM. The proper frequency band in Figure 8(a) is low and at the range of rotating frequency. The amplitude spectrum of the envelope signal was calculated using the frequency band obtained from the kurtogram, as shown in Figures 10 and 11. One can see that they are similar at 3600 RPM and 5000 RPM. However, the amplitude spectrum in Figure 10(a) has a low signal-to-noise ratio at 1800 RPM due to the low center frequency in Figure 10(a). The BPFI can be seen from the amplitude spectrum. However, the rotating frequency and its harmonics also play a major role in the amplitude spectrum, which may hinder identification of the BPFI. Compared Figure 10 with Figure 8 and Figure 11 with Figure 9, one can see that the identification of BPFI is not as obvious as that of BPFO.

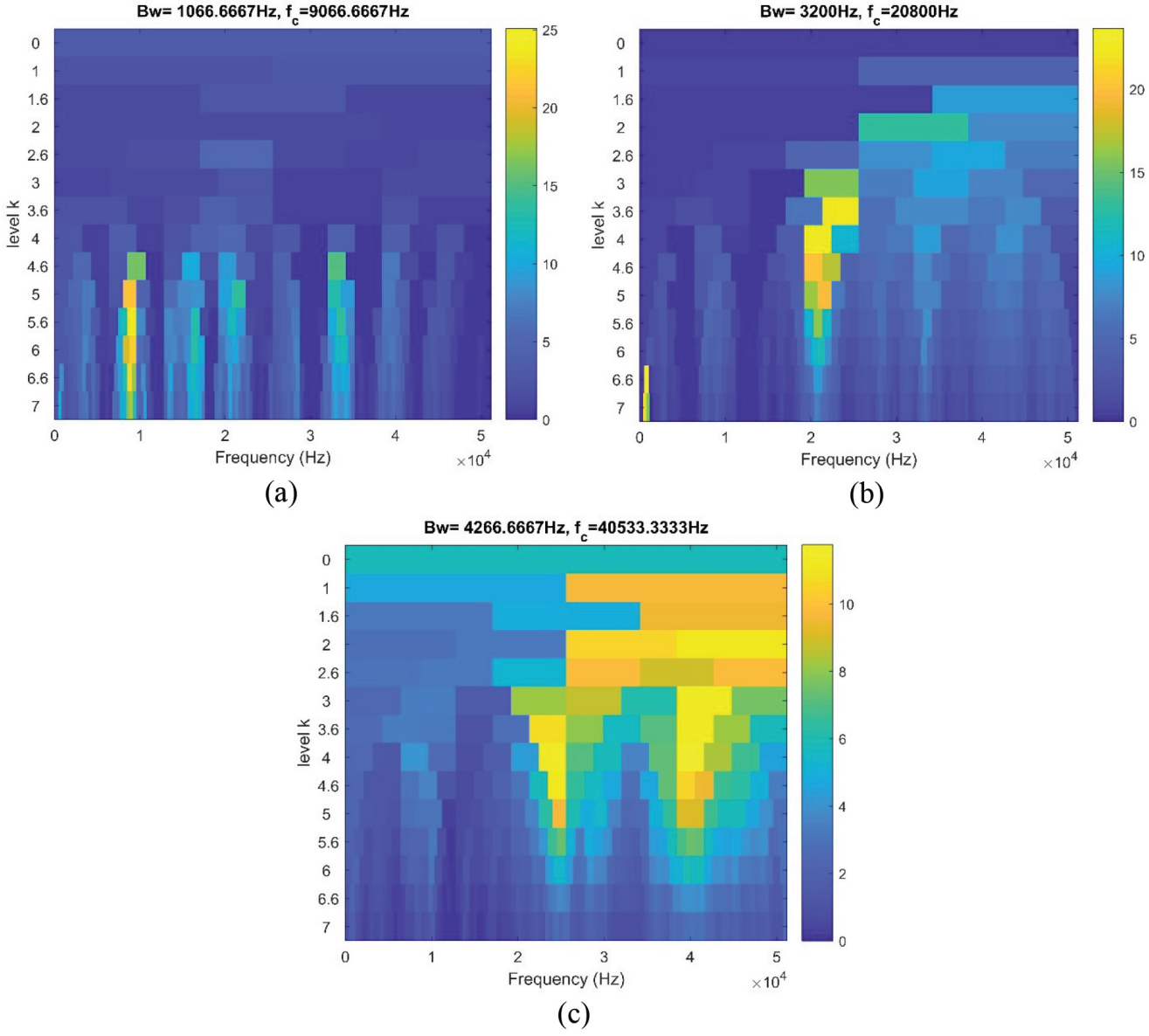



**Fig. 10** Kurtogram corresponding to the inner race fault at (a) 1800 RPM, (b) 3600 RPM and (c) 5000 RPM calculated by the fast algorithm

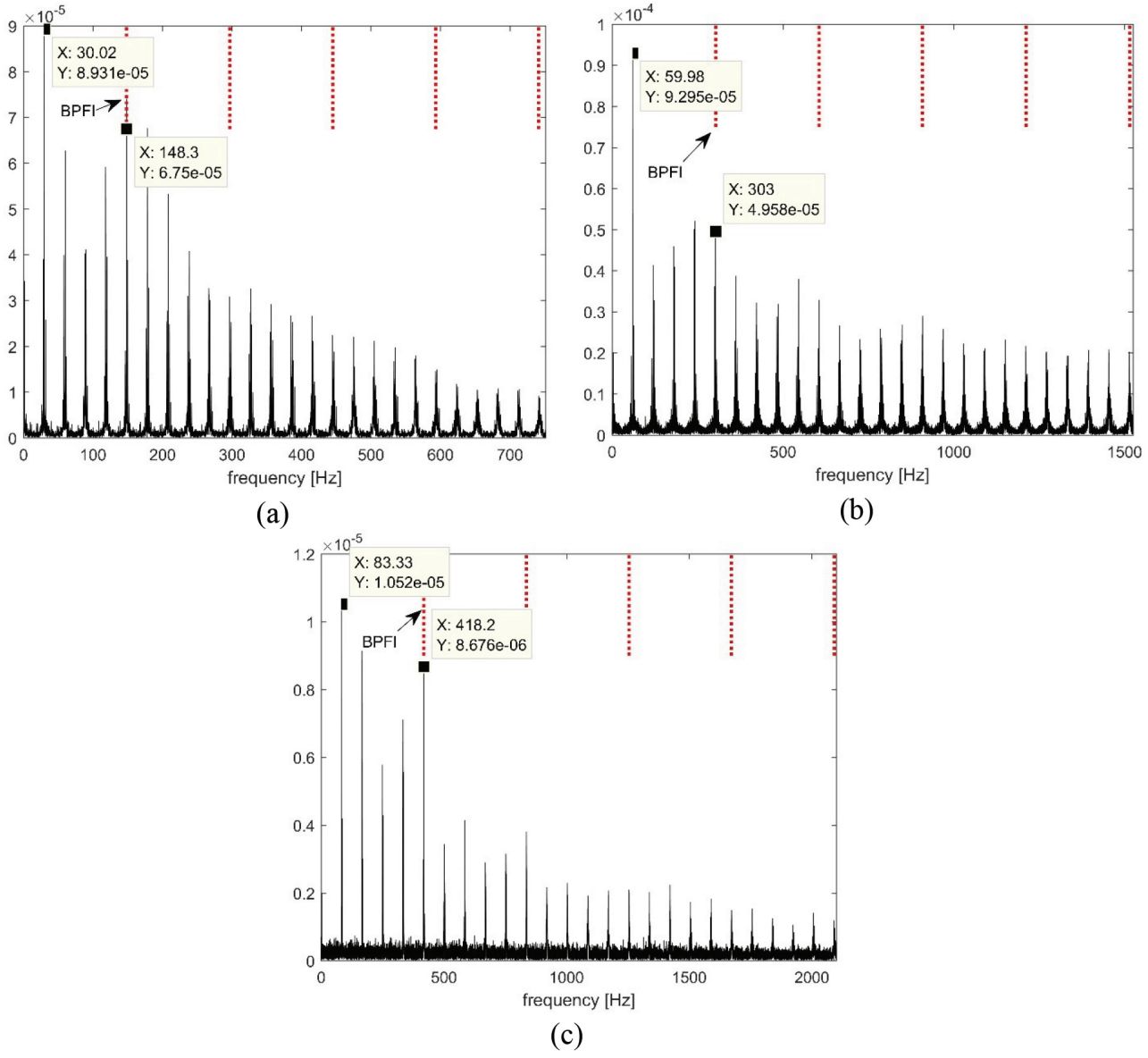



**Fig. 11** Amplitude spectrum of the square envelope signal from the fast algorithm corresponding to the inner race fault at (a) 1800 RPM, (b) 3600 RPM and (c) 5000 RPM

## Conclusion

Fault analysis of rolling element bearings using MED and SK is presented in this paper. A brief introduction of the methodology is given. Experiments on a drive-train test rig were conducted to investigate the methodology. Some observations are summarized as follows:

(1) By maximizing the SK of a measured signal, an inverse filter can be designed by the MED technique to reduce the effect of the transfer path on the measured signal.
(2) The kurtogram can help select a proper frequency band for envelope analysis. Two methods to calculate the kurtogram are investigated in this paper. Though the frequency bands obtained from the wavelet method and the fast algorithm are different, the amplitude spectrums of the square envelope signals from the two methods are similar and both of them can be used to identify bearing fault frequencies.
(3) Compared to the BPFO, the rotating frequency and its harmonics have more negative effect on the identification of the BPFI.

The combination of MED and SK shows a great potential for an automated diagnosis procedure to identify rolling element bearing faults.

## References


1. Randall, R. B., & Antoni, J. (2011). Rolling element bearing diagnostics—A tutorial. *Mechanical systems and signal processing*, *25*(2), 485-520.
2. Smith, W. A., & Randall, R. B. (2015). Rolling element bearing diagnostics using the Case Western Reserve University data: A benchmark study. *Mechanical Systems and Signal Processing*, *64*, 100-131.
3. Sawalhi, N. (2007). Diagnostics, prognostics and fault simulation for rolling element bearings. *The University of New South Wales, School of Mechanical and Manufacturing Engineering, Australia, Doctor of Philosophy thesis*.
4. Randall, R. B., Sawalhi, N., & Coats, M. (2011). A comparison of methods for separation of deterministic and random signals. *International Journal of Condition Monitoring*, *1*(1), 11-19.
5. Endo, H., & Randall, R. B. (2007). Enhancement of autoregressive model based gear tooth fault detection technique by the use of minimum entropy deconvolution filter. *Mechanical Systems and Signal Processing*, *21*(2), 906-919.
6. Sawalhi, N., Randall, R. B., & Endo, H. (2007). The enhancement of fault detection and diagnosis in rolling element bearings using minimum entropy deconvolution combined with spectral kurtosis. *Mechanical Systems and Signal Processing*, *21*(6), 2616-2633.
7. Antoni, J. (2006). The spectral kurtosis: a useful tool for characterising non-stationary signals. *Mechanical Systems and Signal Processing*, *20*(2), 282-307.
8. Antoni, J., & Randall, R. B. (2006). The spectral kurtosis: application to the vibratory surveillance and diagnostics of rotating machines. *Mechanical systems and signal processing*, *20*(2), 308-331.
9. Antoni, J. (2007). Fast computation of the kurtogram for the detection of transient faults. *Mechanical Systems and Signal Processing*, *21*(1), 108-124.